Case Studies in Construction Materials 17 (2022) e01479

Contents lists available at ScienceDirect

Case Studies in Construction Materials

journal homepage: www.elsevier.com/locate/cscm

Investigation of color pigment incorporated roller compacted high performance concrete as a mitigation tool against urban heat island

Gokhan Calis [a,*], Sadik Alper Yildizel [a], Ulku Sultan Keskin [b]

[a] Karamanoglu Mehmetbey University, Karaman, Turkey
[b] Konya Technical University, Konya, Turkey

ARTICLE INFO

Keywords:
Urban heat island
Roller compacted high performance concrete
Cool pavement
Colored concrete
Pigment
Reflective pavement

ABSTRACT

Traditional asphalt pavement is one of the causes of urban heat island due to its low albedo. Although the use of various pavement materials is widely preferred method to mitigate urban heat island effect, the use of color pigment added roller compacted high performance concrete as road pavement is a new approach. Within the scope of this research color pigment incorporated roller compacted high performance concrete (CIP-RCHPC) was produced to mitigate urban heat island. Color pigment was used at the rate of 0.25 % 0.5 % 0.75 % and 1 % of cement by weight. Vebe, compressive strength, splitting tensile strength and albedo determination tests were performed on the samples. Highest albedo was obtained as 0.69 on the RCHPC sample that containing color pigment 0.75 % of cement by weight. A selected area was modeled in ENVI-met software with two configurations. In the base configuration road pavement material was set to be asphalt and in roller compacted concrete (RCC) configuration pavement material was set to be RCHPC with 0.69 albedo value. Air temperature, relative humidity, surface temperature and reflected sort wave radiation results were obtained from the both simulations. In the asphalt configuration the highest air temperature was determined to be 33.72 °C while it was determined to be 32.55 °C RCC configuration. Utilization of color incorporated RCHPC as a pavement material results in 1.63 °C decrease on air temperature, 9.69 °C reduce on surface temperature, 8 % increase on relative humidity and 56 % on sort wave reflectance, in the model area which is an ordinary urban area containing residential buildings and streets where speed limit is 50 km/h.

1. Introduction

There is a reciprocal relationship between city and climate. The climate has a direct effect on the way of city development, and the development of city affects the climate [1]. The climate is a determinant of what kind of building is needed within a city, amount of energy consumption, and type of material used in those buildings. The temperature in the city centers is generally higher than the near rural areas. This can be considered as a result of urbanization, diminishing of great area, low wind velocity due to the high density of building and covering the areas with non-natural materials such as asphalt, curbstone concrete. This situation is defined as Urban Heat Island (UHI) effect [2]. The urban heat island creates several urban microclimates that are characterized by high temperatures and

* Corresponding author.
E-mail addresses: gokhancalis@kmu.edu.tr (G. Calis), sayildizel@kmu.edu.tr (S.A. Yildizel), uskeskin@ktun.edu.tr (U.S. Keskin).

https://doi.org/10.1016/j.cscm.2022.e01479
Received 28 July 2022; Received in revised form 31 August 2022; Accepted 12 September 2022
Available online 15 September 2022

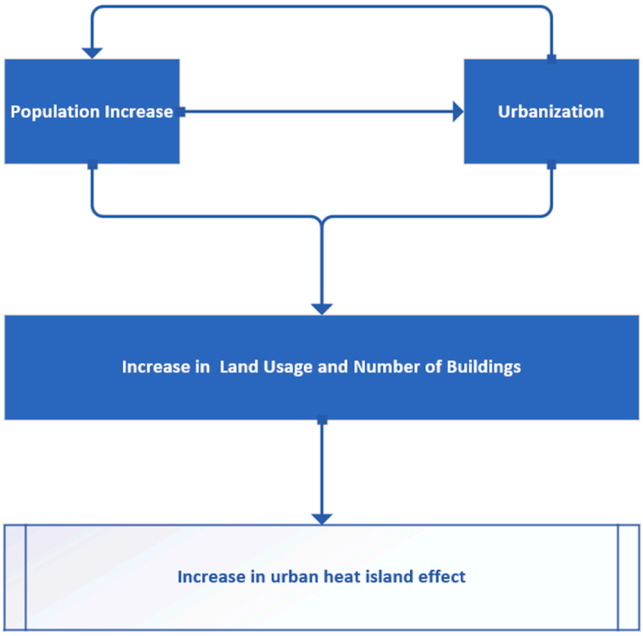

Fig. 1. Urban heat island formation.

Table 1
Color Pigment % by weight of cement.

Color Pigment % by weight of cement	Reference
3–6 %	[80]
2.5–5 %	[81]
1 %, 2 %, 3 %, 4 %, 5 %, 6 %	[82]
1 %, 5 %, 10 %	[83]

Table 2
Mix Design of RCHPC.

Sample	Water (kg)	Cement (kg)	Agg. (0–5 mm) (kg)	Agg. (5–15 mm) (kg)	Agg. (15–25 mm) (kg)	Air (kg)	Curing Additive (kg)	Color Pigment (%)
RCHPC5	110	295	1160	464	408	2.95	5	0
RCHPC6	110	295	1160	464	408	2.95	5	0,25
RCHPC7	110	295	1160	464	408	2.95	5	0.5
RCHPC8	110	295	1160	464	408	2.95	5	0.75
RCHPC9	110	295	1160	464	408	2.95	5	1

density become more pronounced in the center of the city, densely populated and industrial areas [3,4]. World's population live in urban areas is expected to reach 68% by 2050. Urbanization can be seen one of the main and most triggering reason for UHI. The increase in the building stock brought about by urbanization and road coverings lead reduction of natural vegetation, and the placement of materials that absorb heat causes less reflection than natural vegetation [5]. The summary of how urban heat island forms can be seen in Fig. 1.

Causes of UHI can be seen as result of; increase of building stocks and heat emitting surfaces and decrease of vegetation [6–12], road pavement materials [13–15], urban sprawl [16–18], increase of population [19–22].

The heat island density can be determined as the difference between urban heat and rural heat, and this value can be considerably large.In a study conducted in a small town in Greece, it was found that the average UHI density in August reached 3.8 °C during the night while immediate temperature was 5.6 °C [23]. In another study conducted in Italy, it was observed that the temperature raise in winter is 2 °C and 5.2 °C in summer [24]. The intensity of heat difference caused by the UHI effect was also measured in Lisbon, Portugal. It was [25] determined that the temperature difference varied between 0.5 °C and 4 °C as a result of the UHI effect in Lisbon. The heat island effect of temperature raise might be up to 7.5 °C even in a small city located on the coastal area of Portuguese [26].

The size of city population affects urban heat island formation and the heat difference between the city center and the near rural

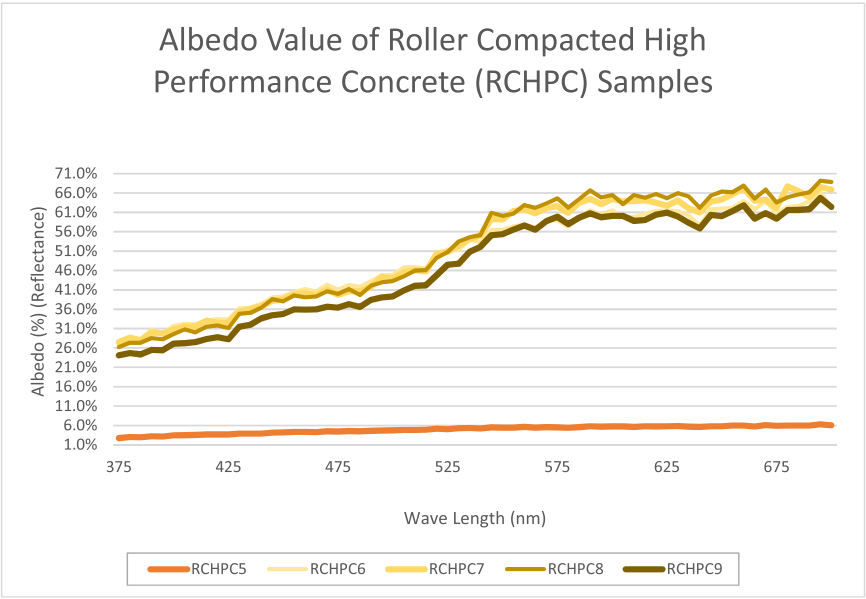

Fig. 2. Albedo Values of RCHPC Samples.

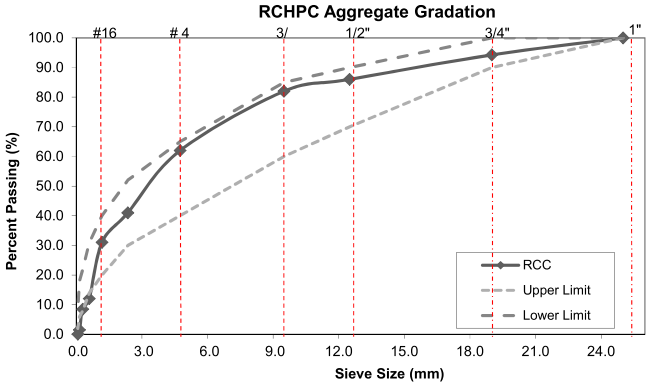

Fig. 3. Aggregate Gradation Curve.

area. This temperature can be 2 °C for a city with a population of approximately 1000, and up to 12 °C for a mega city with a population of several million. The increase in temperature caused by the UHI has many effects on energy consumption, pedestrian comfort, the environment and human health, heat-related deaths [27,28].

UHI is determined to be one of the most effective factors that increases energy consumption in cities [29]. As a result of elevated outdoor temperature energy consumption for cooling indoor temperature can increase up to 4 %. However, energy consumption for cooling can be decreased by 6 % if the outdoor temperature decreases 1 °C at noon. It was determined that monthly cooling energy consumption in dense cities could be 120 % higher than surrounding rural areas[30]. Arifwidodo et al. [31] carried out a research on effects of UHI on buildings energy consumption in far east countries Thailand(Bangkok) and Indonesia(Bandung). According to their findings cities with higher UHI effect consume considerably higher energy than suburban areas. Santamouris [30] proved that during the time period 1970–2010, cooling demand of buildings increased nearly 25 % while heating load decreased 19%. In the city of Athens where UHI leads 10 °C temperature raise, cooling energy consumption of buildings increased 100 % [32]. In dense cities such as Los Angeles and Tokyo, the effect of temperature change on energy consumption was quantified. It was determined that 1 Fahrenheit increase would cause an increase of 300 MW in energy demand in Los Angeles, 1 °C increase would lead 33 GWh increase in building energy consumption in Tokyo [33]. Roxon et al. [34] investigated effects of outdoor air temperature on energy use in the residential buildings in 48 US states for 12 years of time. They emphasize on that depending upon the climate of the state UHI effect can be negative or positive. In the cold regions UHI effect can be positive as it leads a reduction in energy heating consumption consequently carbon foot print would decrease.

Due to increased energy demand of residents for cooling indoor temperature, power plants will generate more electricity that will cause higher air pollution and greenhouse gas emission. This situation would cause ozone formation at the ground level which is main

Tablee 3
Properties of cement.

Chemical and Physical Properties		Upper and Lower Limits as per EN 197–1	
		Min.	Max.
Insoluble Residue	0.17%	–	5
SiO_2	21.61%	–	–
Al_2O_3	4.07%	–	–
Fe_2O_3	0.27%	–	–
CaO	65.71%	–	–
MgO	1.32%	–	–
SO_3	3.34%	–	4
Loss ın Ignition	3.21%	–	5
Na_2O	0.31%	–	–
K_2O	0.34%	–	–
Chloride(Cl^-)	0.01%	–	0.1
Free CaO	1.60%	–	–
Specific Weight	3.06 gr/cm^3	–	–
Specific Surface Area (Blaine)	4600 cm^2/gr	–	–
Initial Setting	100 mnt.	45	–
Final Setting	130 mnt.	–	–
Water	30%	–	–
Volume Consistency (Le Chateller)	1 mm	–	10
Residue in 0.045 mm Sieve	1%	–	–
Residue in 0.090 mm Sieve	0.1%	–	–

Tablee 4
Pigment Properties.

Property	Value	Reference
Size of Particle (325 mesh)	0.54	ASTM D 185
Fe_2O_3	84	ASTM D-50–81
Moisture 105 C°%	0.4	ASTM D-280–33
Oil absorption	54	ASTM D-281
Water soluable salt %	0.6	ASTM D-1208
PH(%5 water solution)	7	
Ignition Lost 1000 C %	13	ASTM D-50
Chemical Formula	$FeO(OH)_nH_2O$	

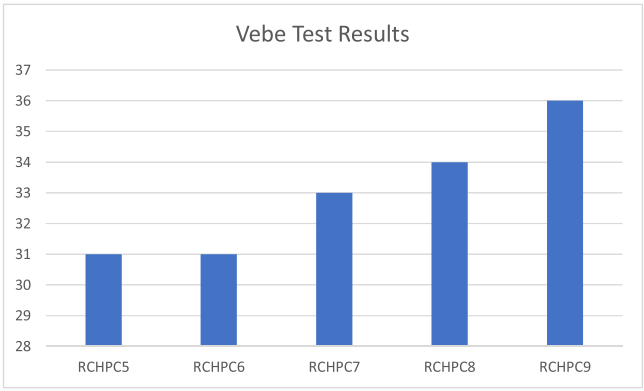

Fig. 4. Vebe Test Results.

Fig. 5. Mechanical tests. Fig. 5**a.** Compressive Strength Test Fig. 5**b.** Splitting Tensile Strength Test.

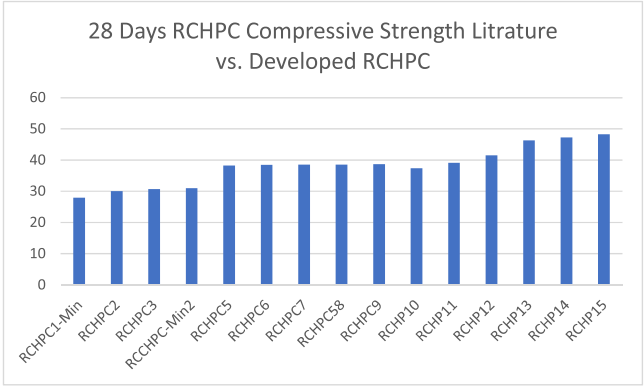

Fig. 6. Compressive Strength Test Results Samples vs. other studies in the literature.

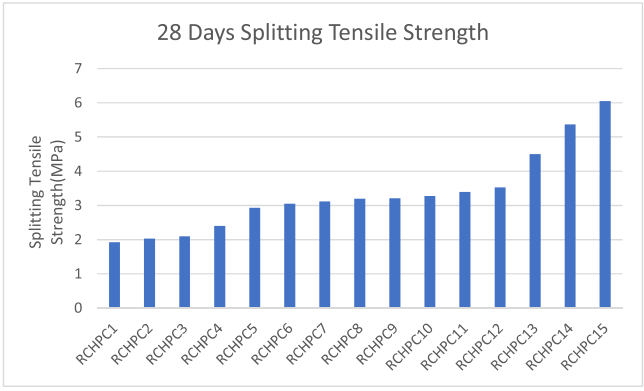

Fig. 7. Splitting Tensile Test Results Samples vs. other studies in the literature.

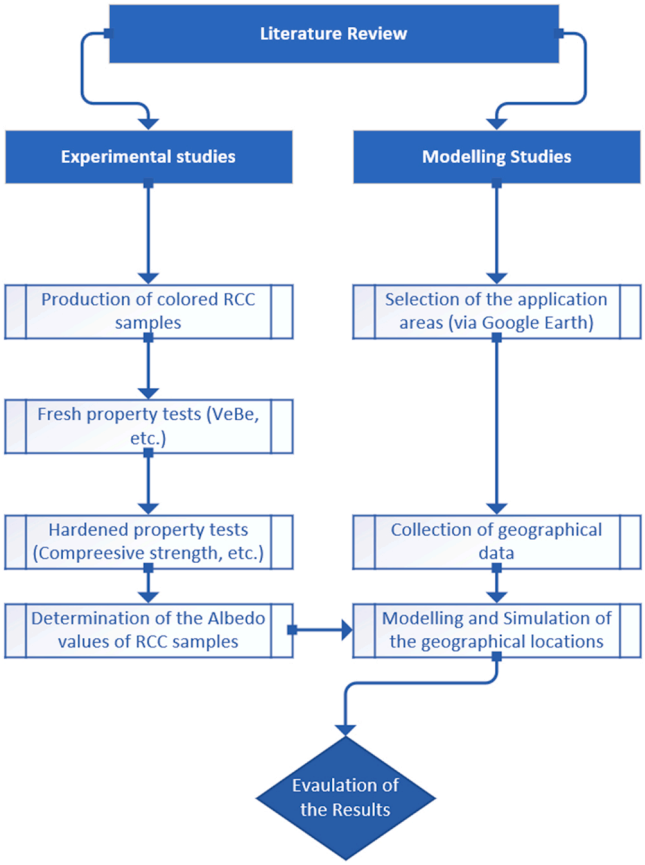

Fig. 8. Flowchart of the research.

Table 5
Boundary Conditions and input data for simulation file in ENVI-met.

	Base configuration	RCC configuration
Latitude-Longitude	37°.87′ N-32°.49′ E	
Climate Type	Hot dry summer	
Grid Boundaries (number of cells)	103×86×36	
Cell Size	dx= 3 m dy= 3 m dz= 4 m	
Wind direction/speed	East/2.5 m/s	
Min/Max Temperature	22–34 °C	
Start Simulation Day	27. Jul.21	
Simulation Start Time	07:00 AM	
Simulation End Time	15:00 PM	
Pavement Material	Asphalt	RCHPC
Albedo of Pavement	0.2	0.69

component of harmful photochemical smog.

Elevated temperature has negative impact on human beings' physical and mental health[35], also reduces human comfort and increases risk of heat related deaths [31,36,37]. Goggins et al. [38] showed that in urban areas where UHI effect is certain, 1 °C increase in air temperature would increase heat related death rates by 4.1%. 4.1 % Another study conducted in Canada indicates that relative mortality rate increases by 2.3 % for each degree increase in air temperature [26].

Fig. 9. UV Spectrophotometer.

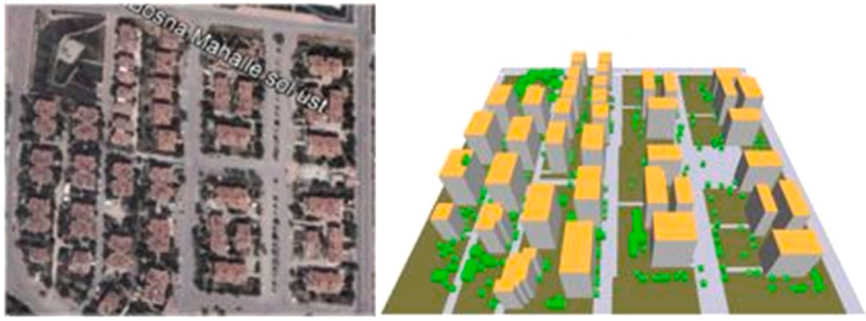

Fig. 10. Model Area.

Table 6
Simulation Results.

		Base (Asphalt) Configuration		RCC Configuration	
Result	Time	Min	Max	Min	Max
Potential Air Temperature	11:00	27.73 °C	30.04 °C	27.56 °C	28.6 °C
	12:00(noon)	28.74 °C	31.56 °C	28.65 °C	29.96 °C
	13:00	29.73 °C	32.74 °C	29.59 °C	31.29 °C
	13:59	30.58 °C	33.72 °C	30.41 °C	32.55 °C
Relative humidity (RH)	11:00	55.00 %	65.21 %	60.88 %	66.00 %
	12:00(noon)	51.96 %	62.06 %	57.81 %	62.72 %
	13:00	50.00 %	59.28 %	55.28 %	59.92 %
	13:59	48.46 %	57.05 %	52.79 %	57.62 %
Reflected Shortwave (SW) Radiation	11:00	58.81 W/m^2	272.57 W/m^2	101.43 W/m^2	427.28 W/m^2
	12:00(noon)	65.16 W/m^2	304.91 W/m^2	106.34 W/m^2	455.36 W/m^2
	13:00	67.54 W/m^2	323.72 W/m^2	104.96 W/m^2	458.85 W/m^2
	13:59	62.52 W/m^2	303.32 W/m^2	94.88 W/m^2	421.03 W/m^2
Surface Temperature	11:00	19.85 °C	44.29 °C	19.85 °C	35.04 °C
	12:00(noon)	19.85 °C	49.14 °C	19.85 °C	39.45 °C
	13:00	19.85 °C	51.37 °C	19.85 °C	42.00 °C
	13:59	19.85 °C	51.93 °C	24.82 °C	43.52 °C

The urban heat island effect has become one of the problems gaining the attention of local and central governments. Although many precautions have been taken, the problem still remains unsolved. Mostly known mitigation strategies are; creation of surfaces with high albedo value [6], water evaporation from rough surfaces [40,41], evaporation of water at ground level [42], evaporation of water from roof gutters [43], vegetation on surfaces, planting on roofs/terraces [44] and afforestation [45,46]. On the other hand, changing the material properties is another measure that can be taken for the UHI effect. Materials suitable for this situation are called “cool materials”. Cool materials; may be reflective, permeable, covered with light grass [15,47–49]. In the recent studies it was determined that pavements have determining effect on overall urban thermal conditions and urban heat island. Furthermore, increasing albedo of pavement or utilization of high albedo pavement can contribute lowering urban heat island effect and air temperature in urban areas [50,51]. Cold pavements mainly contain materials that offer high albedo and high reflectivity and high thermal emittance [52].

Pavement absorbs the heat during the day time, and radiates the heat during at night. When the incoming solar radiation heats the

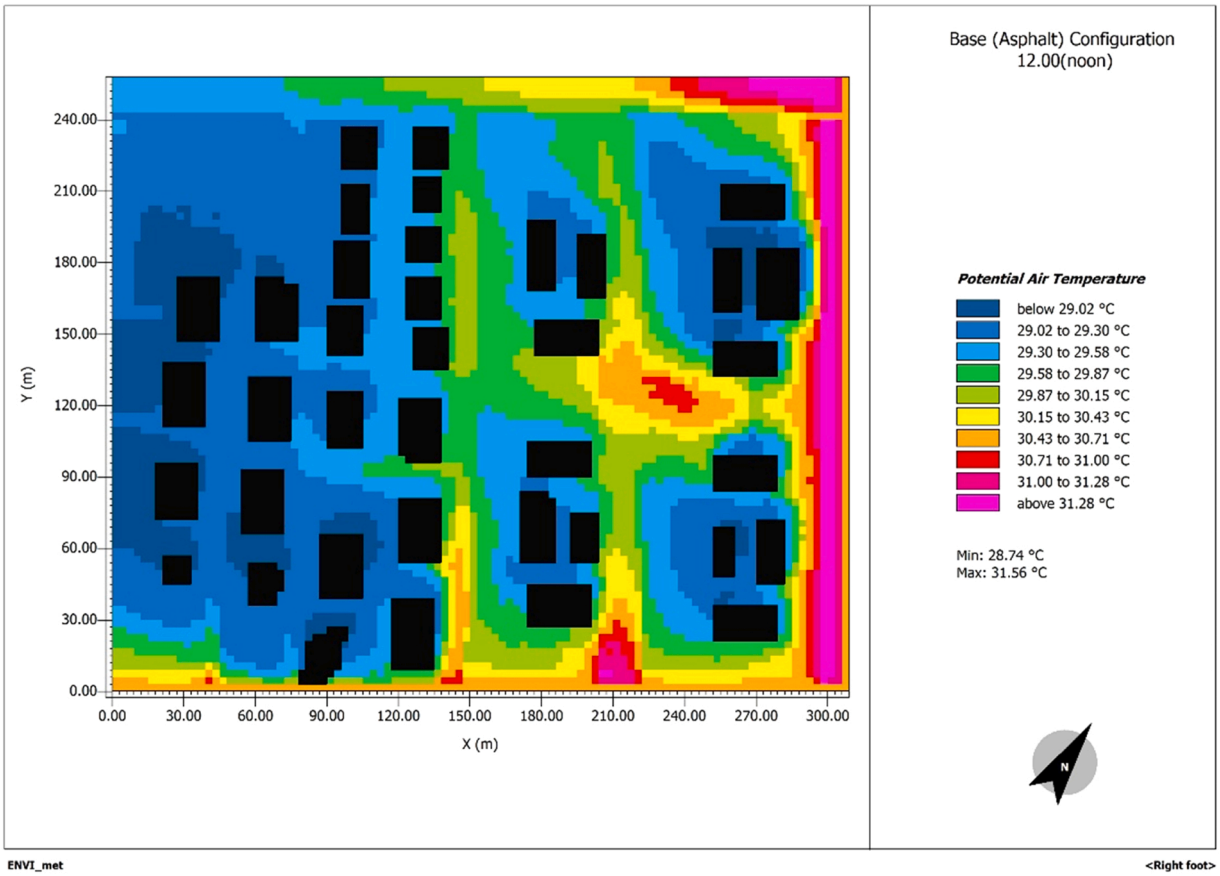

Fig. 11. Potential Air Temperature Asphalt Pavement.

asphalt surface, surface temperature might go up to 67 °C [53–55]. In the recent study it was proved that if albedo of pavement increases 0.1, maximum surface temperature can be reduced by 6 °C [56]. Synnefa et al. [57] prepared five different color pigment added asphalt layers and observed their effects on the air temperature. Temperature of asphalt surface can be reduced by 16–24 °C during the day 2 °C in the night time. Karlessi et al.[58] utilized color changing paints on concrete pavements in their research and achieved reduce of surface temperature by 5.4 °C during the day.

In the recent study effect of a building position and building cladding material were investigated by site measurements and ENVI-met simulation software [59]. The difference between site measurement and ENVI-met results were determined to be 5 %. In the other study [60] impacts of building façade model and material on urban heat island were investigated by modeling in ENVI-met and the significance of façade material on UHI was presented. ENVI-met have been compared to other software and reliability of ENVI-met results have been proved [61,62].

Even though mechanical properties of high performance concrete [63–65], coating surfaces [53,66–69] were examined, there is no scientific research investigating color pigment added roller compacted high performance concrete pavement [70], and its utilization as a mitigation tool against UHI. There are numerous researches [71–75] in which cool pavement and effect of surface's albedo on UHI via ENVI-met were examined in the literature. In this study it was aimed to produce color pigment incorporated roller compacted high performance concrete (CPI-RCHPC) with high reflectivity, to explore effect of utilization of RCHPC as a mitigation tool and to discover what advantages it might provide compared to asphalt pavement. With this respect this research is unique and brings a new approach to mitigate urban heat island effect.

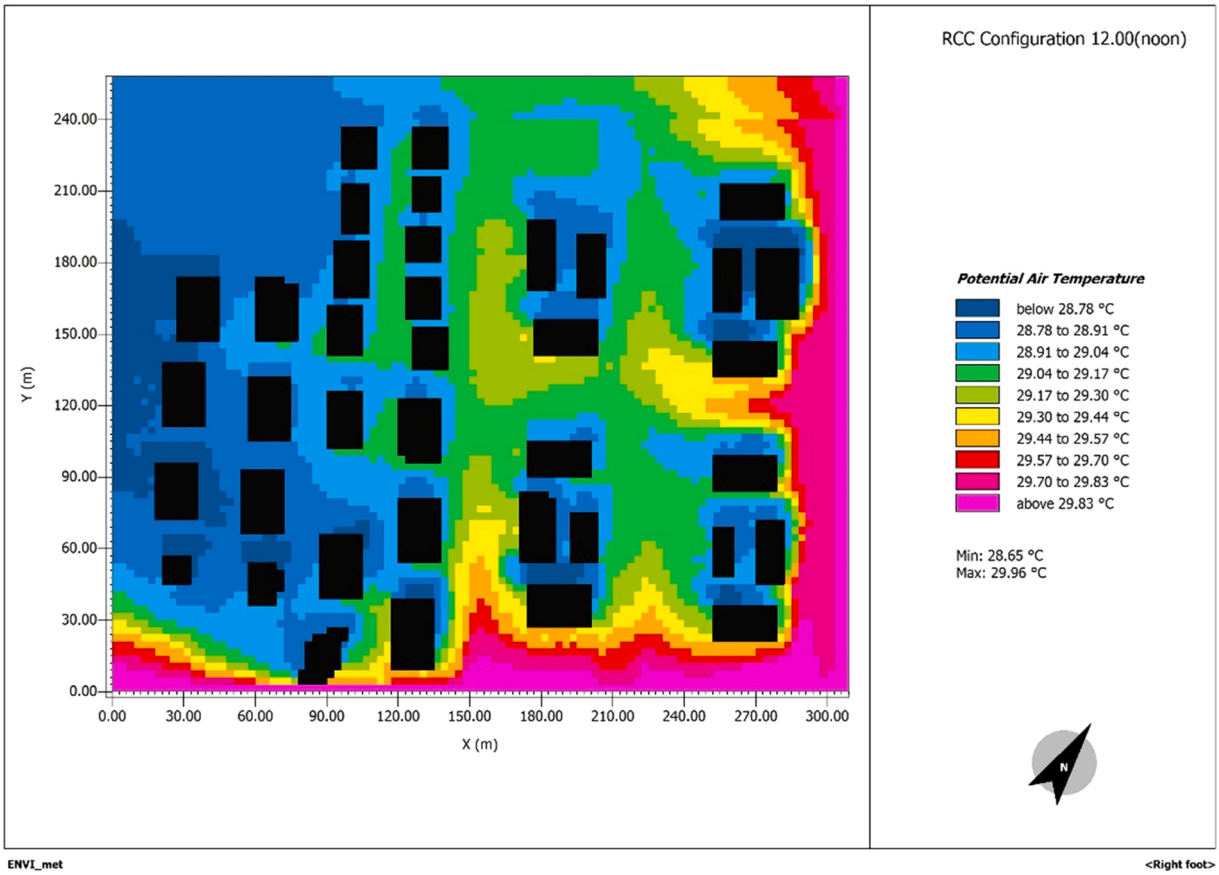

Fig. 12. Potential Air Temperature color pigment added RCHPC pavement.

2. Materials and methodology

2.1. Materials

Roller compacted concrete (RCC) is utilized mainly in dams and roads. RCC became commonly preferred practice as pavement material especially in the urban areas [76]. RCC contains exactly same elements as the conventional concrete which are aggregates, cement-based material and water. The main thing differentiates RCC from normal concrete is the portion of the materials. RCC contains higher volume of fine aggregate than conventional concrete [77]. Cement is approximately 15% by weight in conventional concrete, while it is around 12 % in RCC. Type of cement has vital impact on the hydration process and strength of the concrete in RCC as it has in conventional concrete. Therefore, Portland cement type 2 is mainly preferred due to its ability to generate lower heat at early ages and its longer set times. [78]. With the proper mixture design and compaction works performed at site RCC can develop high level of durability and mechanical performance. Furthermore in the recent study Yildizel et al. indicates that cement replacement materials such as ground calcium carbonate along with fiber improve properties of roller compacted high performance concrete [79].

In the literature scholars have used various amount of color pigments in concrete starting from 1% up to 10% by weight of concrete. Relevant studies from the literature are presented in the Table 1 below.

Concrete mixtures design is presented in the Table 2. The cement amount and water/binder ratio are the same in all the mixtures. In order to select the correct color pigment literature was investigated and yellow pigment was chosen as it has higher reflectance than other colors[84]. Five types of mixtures have been developed. RCHPC5 is control sample and has no pigment, RCHPC6, RCHPC7, RCHPC8 and RCHPC9 have respectively 0.25 %, 0.5 %, 0.75 % and 1 % pigment by weight of cement.

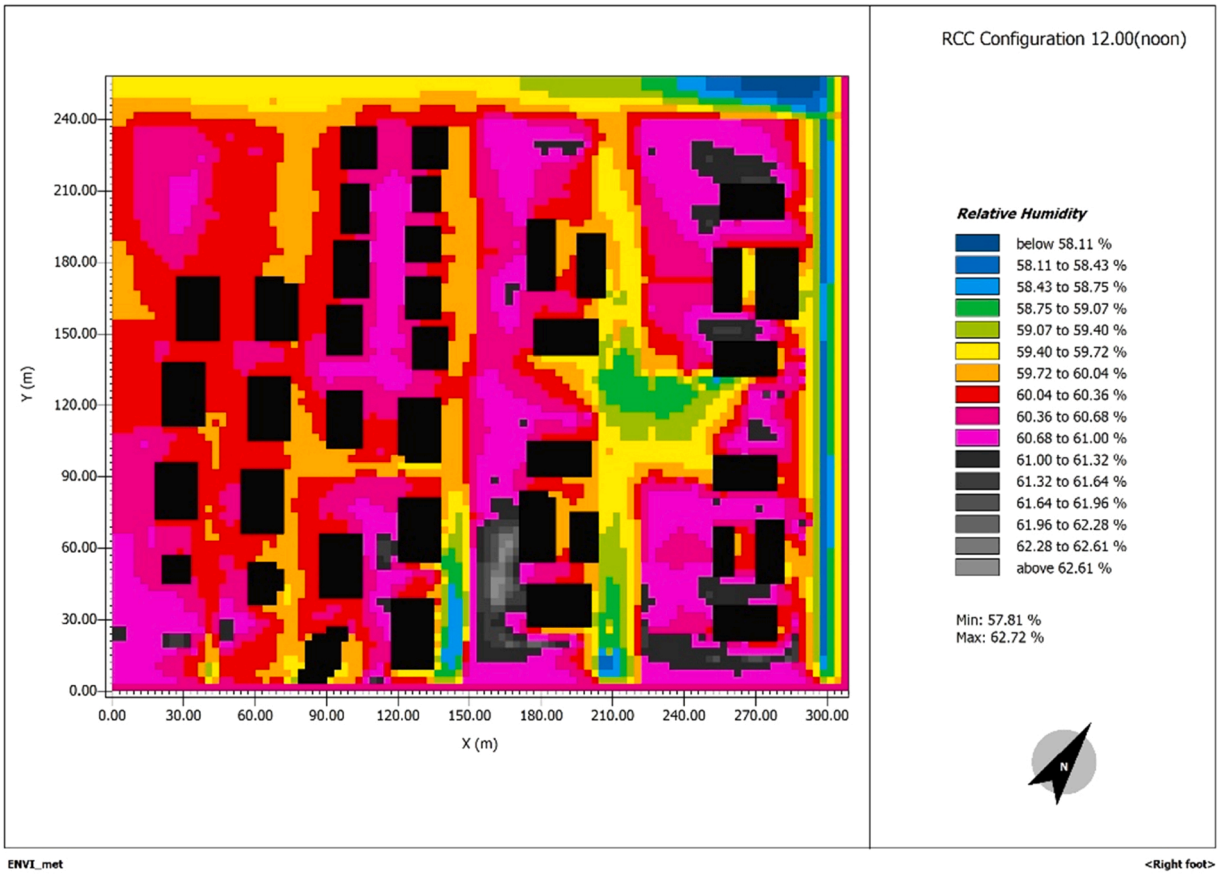

Fig. 13. Relative humidity Asphalt Pavement.

Albedo values of the samples are 0.06, 0.62, 0.67, 0.69 and 0.62. The highest albedo value was determined to be 0.69 on RCHPC8 that contains %0.75 yellow pigment by weight of cement. As it can be seen in the Fig. 2, beyond 0.75 % adding more pigment makes the concrete darker and consequently decreases reflectivity.

The gradation curve of utilized aggregate is presented in the Fig. 3 below.

Chemical and physical properties of cement utilized in the laboratory studies are presented in the Table 3 below. Properties of utilized cement take place in between minimum and maximums values as per EN 197–1.

Properties of pigment are given in Table 4 below. Pigment properties meet the requirements as per relevant standard given in the Table 4.

Fresh state property of RCHPC is determined by vebe test according to ASTM C1170 [85]. Vebe test results are given in Fig. 4.

Compressive and splitting tensile strength tests were performed on RCHPC samples developed in the laboratory. Compressive strength test was performed according to ASTM C39 /C39M [86] and splitting tensile test was performed as per ASTM C496/C496M [87]. Photographs of performed mechanical tests are shown in Fig. 5. Same cement/ water ratio, and amount of aggregate were used in all mixtures. Therefore, mechanical properties of produced RCC samples are very close to each other.

28 days compressive strength (CS) test results and literature studies [89–94] are presented in Fig. 6. Minimum compressive strength for RCC without freeze and thaw effect required by American Concrete Pavement Association (2014) [88] is 28 MPa (RCHPC1-Min) while 31 MPa (RCHPC4-Min2) is required for the samples to be exposed to freeze and thaw conditions. 28 days compressive strength test results of the samples RCHPC5, RCHPC6, RCHPC7, RCHPC8, and RCHPC9 are respectively 38.26 MPa, 38.45 MPa, 38.54 MPa, 38.57 MPa, 38.58 MPa. The produced samples (RCHPC5-RCHPC6- RCHPC7- RCHPC8- RCHPC9) samples meet the min. requirements and take place in the range of literature studies.

28 days split tensile strength (STS) test results are shown in Fig. 7. Split tensile strength of developed RCHPC samples are sufficient and in the range of literature studies results [95–98]. Minimum split tensile strength was determined to be 3.05.97 MPa on RCHPC6, and maximum was 3.21 MPa on RCHPC9 in the laboratory study.

2.2. Methodology

As the first step of this study, literature review was carried out. Later on, causes of UHI, and mitigation strategies were identified

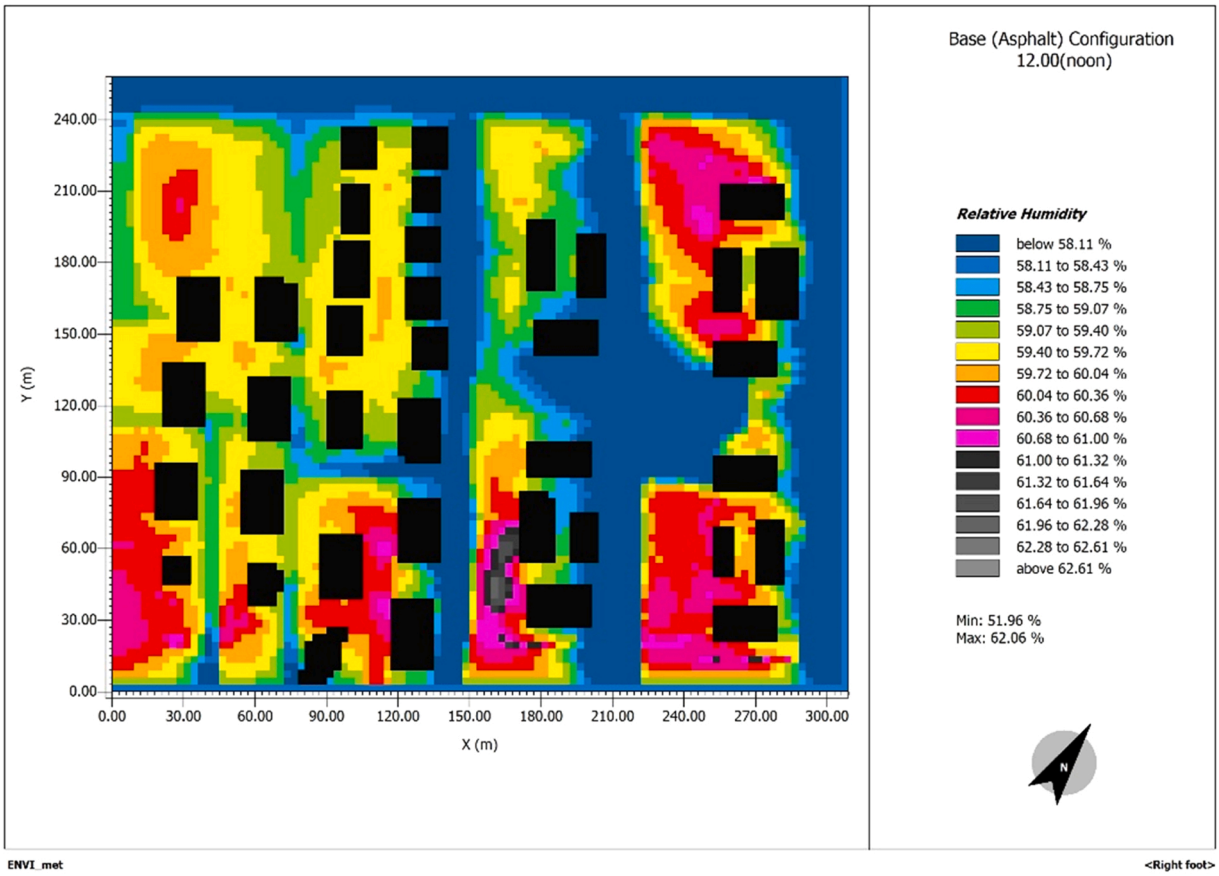

Fig. 14. Relative humidity color pigment added RCC pavement.

from the previous studies. Once literature review was completed experimental and modeling studies started. In the laboratory control mixture RCHPC5 and color incorporated samples (RCHPC6, RCHPC7, RCHPC8 and RCHPC9) were produced. In the fresh state of concrete, vebe test was performed on each sample. In the hardened state 28 days compressive and split tensile strength tests and reflectance (albedo determination) test were carried out. In the modeling phase, an area was selected via Google Earth. Coordinates and geographical data of selected area were obtained. In the last step selected area was modeled with 2 different configurations. In the base configuration road pavement material was set to be an asphalt as per the existing condition of the area. In the second configuration pavement material was set to be color pigment incorporated roller compacted high performance concrete and its albedo value set to be 0.69 which was obtained in the sample RCHPC8. In this sample yellow pigment amount is 0.75 % of cement by weight.

The selected area is 309 m $\times$ 258 and was modeled in ENVI-met for simulation. The area is located in Konya in the central Anatolia region of Turkey. It is nearly 210 km (bird fly distance) away from Mediterranean cost of Turkey. There is terrestrial climate in this region,and also existing urban heat island issues in Konya have been pointed out in the previous studies [99–101]. Fig. 8.

ENVI-met software is computational thermodynamics and fluid dynamics model. In this model RANS equations are used in order to analyze atmospheric flow and heat transfer in urban settings. This model was initially developed by Bruse during his dissertation in Germany in the late 1990′s [102]. In ENVI-met a three dimensional non-hydro-static model is established with the purpose of simulating surfaces (buildings-pavements etc)-plant-air [103]. The interaction between surfaces and plants namely; heat flux around and between buildings,heat and steam exchange at the soil level and between walls, turbulence, thermo-hygrometric exchange in vegetation, bioclimatology, fluid dynamics of small particles and polluting species are structured in the simulation and analyzed [104].

Area input file and project location are two main inputs required for ENVI-met simulation. While the area input file can be generated via other design software such as: sketch-up, rhino, it can also be created within ENVI-met. The area input file must contain type of materials used in the pavements, vegetations, soil materials, buildings, buildings' roof covering material. ENVI-met offers wide range of material library and still, any user can add any type of material with its physical properties.

Within the scope of this study a case, in which 2 configurations take place, was investigated. In the first configuration which called base(asphalt) configuration, the road pavement material is asphalt. Because the current pavement material in the selected area is asphalt and further asphalt is widely used in the cities as road pavement. In the second configuration the pavement material is color pigment incorporated roller compacted high performance concrete. This will be called as "RCC configuration". Boundary conditions of simulation case are given in the Table 5 below.

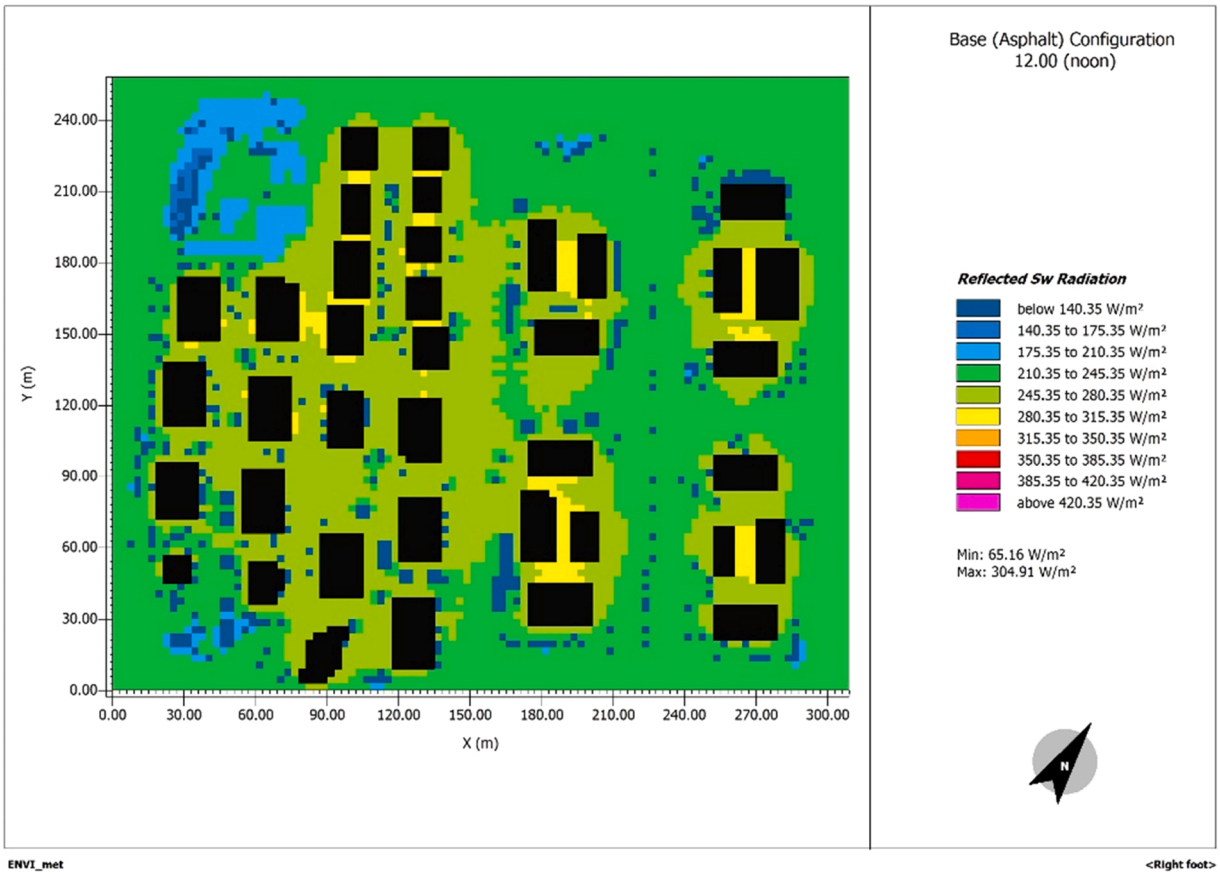

Fig. 15. Reflected SW Radiation Asphalt Pavement.

The spectrophotometer was used to determine albedo value of CPI -RCHPC is presented in Fig. 9. below. Albedo value determination test was performed in accordance with ASTM E903 [105]. Highest albedo of RCHPC was determined to be 0.69 on RCHPC8.

3. Simulation results and discussion

The area image obtained from google maps and model area generated in ENVI-met are shown in Fig. 10. The heights of buildings were determined by reviewing 3D maps. In this area current road pavement is asphalt. There are 38 buildings, trees, grass, playing ground in this neighborhood. All of these were modeled in ENVI-met. The time frame was set to be starting on 07:00 AM and ending 14:59 PM. The software manual suggests to set the first 30 min to be spin up time. There are studies suggesting spin up time to be 1 h [106,107], in this research the first 4 h regarded to be spin up time as it was suggested by Sharmin et al. [108].

Detailed results of simulation for both configurations are presented in Table 6.

Potential air temperature results of ENVI-met can be seen in Fig. 11 and Fig. 12. In the base (asphalt) configuration minimum air temperature was determined to be 27.73 °C at 11:00 am, 28.74 °C at midday, 29.73 °C at 13:00 and 30.58 °C at 13:59, while the maximum temperatures were 30.04 °C, 31.56 °C, 32.74 °C and 33.72 °C respectively. The RCC configuration on the other hand indicates certain advantage. For the same time frame minimum temperatures are; 27.56 °C, 28.65 °C, 29.59 °C, 30.41 °C while maximum temperatures are 28.6 °C, 29.96 °C, 31.29 °C and 32.55 °C. These results of this study show similarity with the previous studies [75,109–112] in which, changing albedo of asphalt pavement was investigated. In their study Salata et al. [112] was able to reduce air temperature 0.4 °C, Kyriakodis and Santomouris [75] 1.5 °C, Taleghani and Berardi (2017) 0.4 °C in cold climate [109].

In other research effect of shrub was investigated and according to the results it was concluded that increasing shrub has no positive

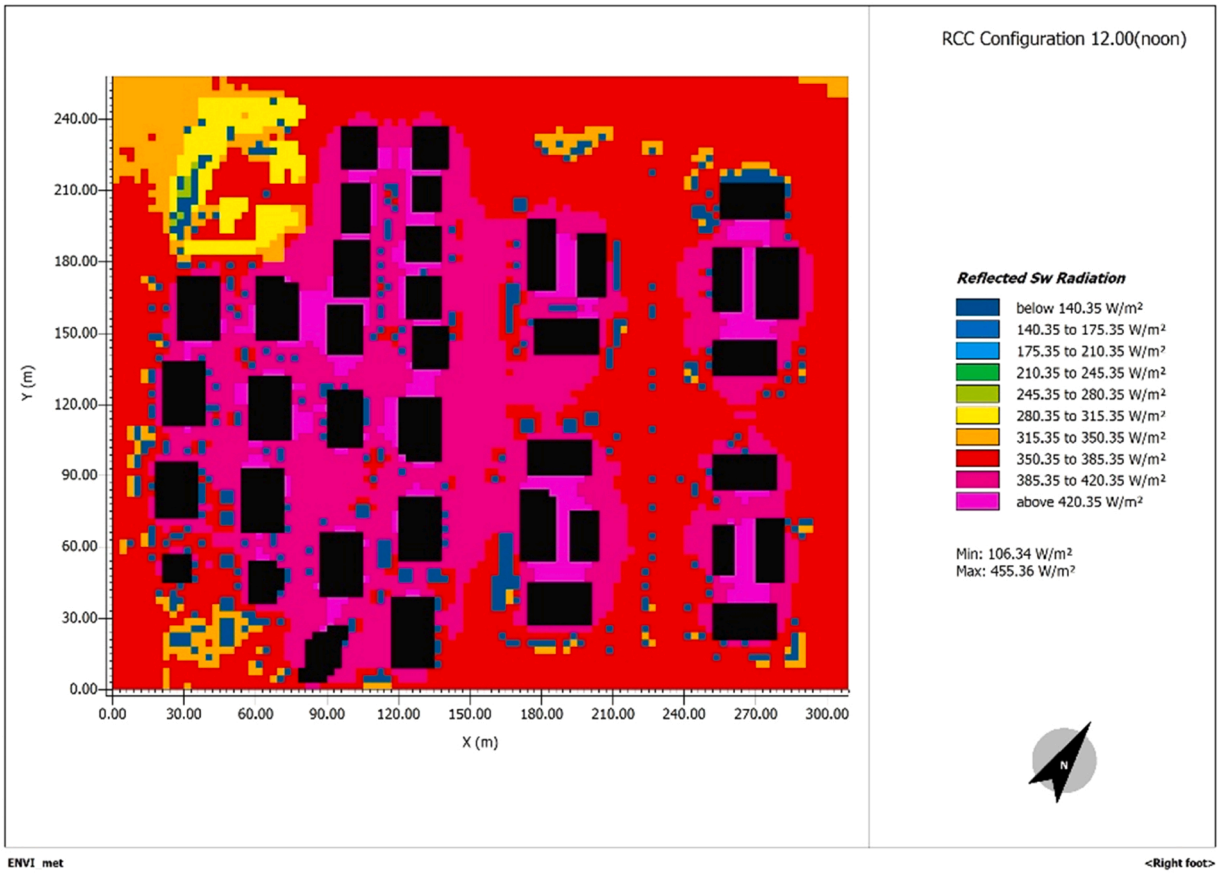

Fig. 16. Reflected SW Radiation color pigment added RCC Pavement.

effect on air temperature [113]. Within the scope of the study carried out in France, the heat exchange caused by irrigation of asphalt pavements was investigated. It was observed that the wetting of the coatings had a temperature drop of 0.79 °C − 0.57 °C and 1.0 °C - 2.3 °C relative to the reference point [114]. Green roof application has proved that air temperature can be reduced up to 0.7 °C [115] while in this study the highest air temperature reduction was determined to be 1.6 °C.

Relative humidity results are presented in Fig. 13 and Fig. 14. Maximum RH results for two configurations are similar to each other. However, in RCC configurations the minimum RH results are higher than asphalt configuration. Minimum RH in RCC configuration is 5.88 % higher than base (asphalt) configuration at 11:00 am, 5.85 % higher at noon, 5.28 % higher at 13:00 % and 4.33 % higher at 13:59. CPI-RCHPC mostly increases the minimum RH level in comparison to asphalt. Berardi et al. found that enhancement of greenery can lead an increment of RH by 7 % [116] which is higher than this study.

Salata et al. [112] have tried 5 configurations with various pavement materials, building coating materials and vegetation in the selected area. They observed that minimum RH changes depending upon the pavement material and cladding while maximum RH is close to each other.

CPI -RCHPC is highly reflective due to its high albedo and optical properties. Reflected SW radiation results are given in Fig. 15 and Fig. 16. RCC reflection is 1.63 times of asphalt for the minimum, and 1.49 times for maximum at noon time. Maximum reflected SW radiation of RCC is 458.85 W/m^2 at noon, while it is 323.72 W/m^2 in asphalt configuration at 13:00.

Fig. 17 shows surface temperature results of 12:00 (noon) for base(asphalt) configuration and Fig. 18 results of RCC configuration.

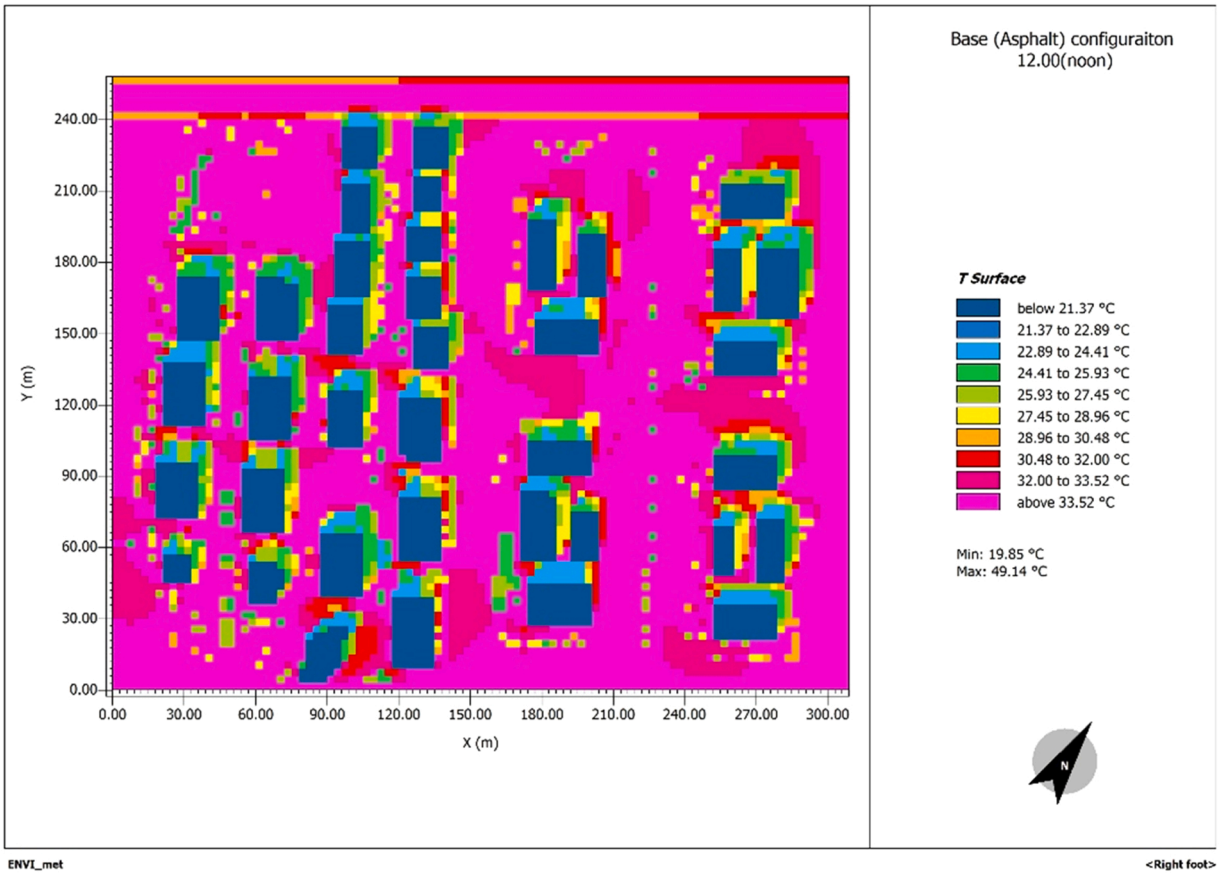

Fig. 17. T Surface Asphalt Pavement.

The surface temperature difference between RCC configuration and asphalt base was determined to be 9.69 °C at noon. The surface temperature of RCHPC is 42.00 °C while the surface of asphalt is 51.37 °C and the variance is 9.37 °C at 13:00. RCHPC has certain advantage over asphalt for the whole simulation time frame. This could be attributed to high albedo value of RCHPC. Lontorfos et al. [117] carried out a researching investigating mitigation performance of reflective pavements. Once conventional asphalt was replaced with reflective concrete pavement surface temperature was determined to be 12.7 °C less than conventional concrete.

Utilization of color pigment added RCHPC pavement decreases T-surface and this results is consistent with other studies in the literature [110,112,118].

4. Conclusion and further work

In this study color pigment incorporated roller compacted high performance concrete was developed. Mechanical, vebe and albedo determination tests were carried out on the samples. In the simulation stage utilization of color pigment added roller compacted high performance concrete as UHI mitigation strategy was evaluated. Potential air temperature, relative humidity, reflected SW radiation and T surface are standard metrics used to determine efficiency of urban heat island mitigation methods.

The following findings obtained from this research:

1. Color pigment incorporation has tiny impact on mechanical properties on roller compacted high performance concrete samples. However, test results of pigment incorporated samples still comply with the minimum requirements defined in the relevant standards.
2. Due to its reflectivity properties of CPI-RCHPC air temperature can be decreased by 1.6 °C at noon time in comparison to the asphalt pavement used scenario. The difference determined to be 1.17 °C at 13:59. It can be deduced that this decrease could easily lead 5–8% decrease in electricity consumption for air conditioning in the selected area. With less electricity consumption less CO_2 emission can be achieved. In this respect CPI-RCHPC would contribute to sustainability at significant level as it reduces consumption of natural resources. Furthermore, once air temperature is reduced by utilization of CPI-RCHPC as road pavements, heat related health issues can be decreased. This would provide substantial benefits to quality of daily life of people at all ages.

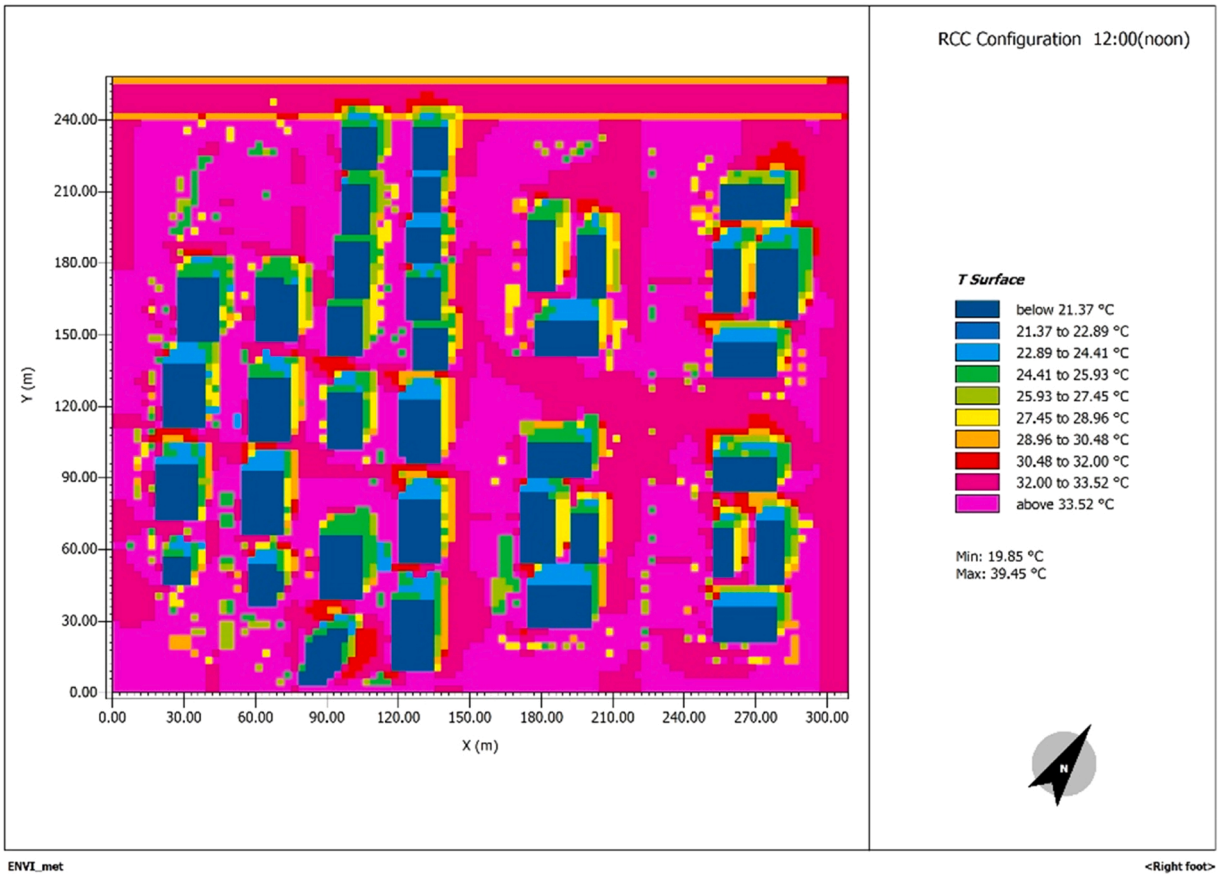

Fig. 18. T Surface color pigment added RCC Pavement.

3. Utilization of color pigment in roller compacted high performance concrete significantly increases albedo value of concrete up to 0.75 % by weight of cement. With higher albedo CPI-RCHPC reflects more SW radiation than conventional asphalt pavement.
4. Utilization of CPI-RCHPC has slight increase on maximum relative humidity. However, minimum level of relative humidity can be increased up to 60.88 %.
5. Highest decrease on surface temperature determined to be 9.69 °C at noon while the minimum decrease is 8.41 °C on 13:59.

CPI-RCHPC developed in this research is certainly advantageous material against urban heat island. However, in this research only color pigment incorporated RCHPC and asphalt were modeled and compared with each other. On the other hand, combination of more mitigation strategies such as green roofs, afforestation along with CPI-RCHPC might be more effective in dealing with urban heat island effects. Furthermore, how much cost can be saved by utilization of CPI-RCHPC due to decrease on electricity consumption was not quantified. These could be subject of future studies.

Declaration of Competing Interest

The authors declare that they have no known competing financial interests or personal relationships that could have appeared to influence the work reported in this paper.

Data availability

Data will be made available on request.

Acknowledgment

This research has been carried out with the support of Konya Technical University Scientific Research Projects Coordinatorship under Project Number of 21104015. The authors would like to thank Konya Technical University for their support.

References

[1] T.B. Kleerekoper, L. Esch, M.V. Salcedo, How to make a city climate-proof, addressing the urban heat island effect, Resour. Conserv. Recycl. 64 (2012) 30–38.
[2] H. Bahi, H., Mastouri, H., Radoine, 1-s2.0-S2214785320320526-main.pdf, Mater. Today Proc. 27 (2020) 3004–3009.
[3] E.N. Adinna, E.I. Christian, A.T. Okolie, Assessment of urban heat island and possible adaptations in Enugu urban using landsat-ETM, J. Geogr. Reg. Plan (2009).
[4] M. Santamouris, C. Cartalis, A. Synnefa, D. Kolokotsa, On the impact of urban heat island and global warming on the power demand and electricity consumption of buildings – a review, Energy Build. (2015), https://doi.org/10.1016/j.enbuild.2014.09.052.
[5] M. Carpio, Á. González, M. González, K. Verichev, Influence of pavements on the urban heat island phenomenon: a scientific evolution analysis, Energy Build. 226 (2020), 110379, https://doi.org/10.1016/j.enbuild.2020.110379.
[6] H. Akbari, M. Pomerantz, H. Taha, Cool surfaces and shade trees to reduce energy use and improve air quality in urban areas, Sol. Energy 70 (2001) 295–310, https://doi.org/10.1016/S0038-092X(00)00089-X.
[7] L. Doulos, M. Santamouris, I. Livada, Passive cooling of outdoor urban spaces. The role of materials, Sol. Energy 77 (2004) 231–249, https://doi.org/10.1016/j.solener.2004.04.005.
[8] F. Cotana, F. Rossi, M. Filipponi, V. Coccia, A.L. Pisello, E. Bonamente, A. Petrozzi, G. Cavalaglio, Albedo control as an effective strategy to tackle global warming: a case study, Appl. Energy 130 (2014) 641–647, https://doi.org/10.1016/j.apenergy.2014.02.065.
[9] M. Santamouris, G.Y. Yun, Recent development and research priorities on cool and super cool materials to mitigate urban heat island, Renew. Energy 161 (2020) 792–807, https://doi.org/10.1016/j.renene.2020.07.109.
[10] S.K.Yusuf, N.H. Wong, E. Hagen, R. Anggoro, Y. Hong, The influence of land use on the urban heat island in Singapore, Habitat International, 31 (2007) 232–242. https://doi.org/10.1016/j.habitatint.2007.02.006.
[11] C. O'Malley, P. Piroozfar, E.R.P. Farr, F. Pomponi, Urban Heat Island (UHI) mitigating strategies: a case-based comparative analysis, Sustain. Cities Soc. 19 (2015) 222–235, https://doi.org/10.1016/j.scs.2015.05.009.
[12] C. Smith, G. Levermore, Designing urban spaces and buildings to improve sustainability and quality of life in a warmer world, Energy Policy 36 (2008) 4558–4562, https://doi.org/10.1016/j.enpol.2008.09.011.
[13] M. Takebayashi, H. Moriyama, Study on surface heat budget of varioud pavements for urban heat island mitigation, Adv. Mater. Sci. Eng. (2012)) (2012), https://doi.org/10.1155/2012/523051.
[14] K.E. Golden, J.S. Kaloush, Mesoscale and microscale evaluation of surface pavement impacts on the urban heat island effects.pdf, Int. J. Pavement Eng. (2006), https://doi.org/10.1080/10298430500505325.
[15] P.E. Phelan, K. Kaloush, M. Miner, J. Golden, B. Phelan, H. Silva, R.A. Taylor, Urban heat island: mechanisms, implications, and possible remedies, Annu. Rev. Environ. Resour. 40 (2015) 285–307, https://doi.org/10.1146/annurev-environ-102014-021155.
[16] B. Stone, J.J. Hess, H. Frumkin, Urban Form and Extreme Heat Events: Are Sprawling Cities More Vulnerable to Climate Change Than Compact Cities? Environmental Health Perspectives 118 (2010) 1425–1428. https://doi.org/10.1289/ehp.0901879.
[17] R. Singh, Urban sprawl and its impact on generation of urban heat island: a case study of Ludhiana city, J. Indian Soc. Remote Sens. 47 (2019) 1567–1576, https://doi.org/10.1007/s12524-019-00994-8.
[18] X. Xu, H. Cai, Z. Qiao, C. Jin, Y. Ge, L. Wang, F. Xu, Impacts of Park Landscape Structure on Thermal Environment Using QuickBird and Landsat Images, Chinese, Geograohical Science 27 (2017), https://doi.org/10.1007/s11769–017-0910-x.
[19] R. Karl, N. Carolina, Wei-Chyung Sciences State University ' During those, 17 (1990) 2377–2380.
[20] N. Debbage, J.M. Shepherd, Computers, environment and urban systems the urban heat island effect and city contiguity, CEUS 54 (2015) 181–194, https://doi.org/10.1016/j.compenvurbsys.2015.08.002.
[21] S. Grimmond, Urbanization and global environmental change: local effects of urban warming, Geogr. J. 173 (2007), https://doi.org/10.1111/j.1475-4959.2007.232_3.x.
[22] L.W. Siu, M.A. Hart, Quantifying urban heat island intensity in Hong Kong SAR, China, Environ. Monit. Assess. 185 (2013) 4383–4398, https://doi.org/10.1007/s10661-012-2876-6.
[23] E. Vardoulakis, D. Karamanis, A. Fotiadi, G. Mihalakakou, The urban heat island effect in a small Mediterranean city of high summer temperatures and cooling energy demands, Sol. Energy 94 (2013) 128–144, https://doi.org/10.1016/j.solener.2013.04.016.
[24] I. Bertocchi, G. Fini, M.C. Rubolino, S. Tondelli, Sustainability achievements in building regulations. the example of Bologna, Procedia Eng. 21 (2011) 957–967, https://doi.org/10.1016/j.proeng.2011.11.2100.
[25] M.J. Alcoforado, H. Andrade, Nocturnal urban heat island in Lisbon (Portugal): main features and modelling attempts, Theor. Appl. Climatol. 84 (2006) 151–159, https://doi.org/10.1007/s00704-005-0152-1.
[26] L. Fahed, J. Kinab, E. Ginestet, S, Adolphe, Impact of urban heat island mitigation measures on microclimate and pedestrian comfort in a dense urban district of Lebanon, Sustain. Cities Soc. (2020).
[27] A. Mohajerani, J. Bakaric, T. Jeffrey-Bailey, The urban heat island effect, its causes, and mitigation, with reference to the thermal properties of asphalt concrete, J. Environ. Manag. 197 (2017) 522–538, https://doi.org/10.1016/j.jenvman.2017.03.095.
[28] R. Giridharan, M. Kolokotroni, Urban heat island characteristics in London during winter, Sol. Energy (2009), https://doi.org/10.1016/j.solener.2009.06.007.
[29] P. Shahmohamadi, A.I. Che-Ani, K.N.A. Maulud, N.M. Tawil, N.A.G. Abdullah, The impact of anthropogenic heat on formation of urban heat island and energy consumption balance, Urban Stud. Res. 2011 (2011) 1–9, https://doi.org/10.1155/2011/497524.
[30] M. Santamouris, N. Papanikolaou, I. Livada, I. Koronakis, C. Georgakis, A. Argiriou, D.N. Assimakopoulos, On the impact of urban climate on the energy consuption of building, Sol. Energy 70 (2001) 201–216, https://doi.org/10.1016/S0038-092X(00)00095-5.
[31] S.D. Arifwidodo, O. Chandrasiri, R. Abdulharis, T. Kubota, Exploring the effects of urban heat island: a case study of two cities in Thailand and Indonesia, APN Sci. Bull. 9 (2019) 10–18, https://doi.org/10.30852/sb.2019.539.
[32] M. Santamouris, On the energy impact of urban heat island and global warming on buildings, Energy Build. 82 (2014) 100–113, https://doi.org/10.1016/j.enbuild.2014.07.022.
[33] N. Asimakopoulos, D.N. Assimakopoulos, V.D. Chrisomallidou, Energy and Climate in the Urban Built Environment, second ed., Taylor & Francis, New York, 2001.
[34] J. Roxon, F.J. Ulm, R.J.M. Pellenq, Urban heat island impact on state residential energy cost and CO_2 emissions in the United States, Urban Clim. 31 (2020), 100546, https://doi.org/10.1016/j.uclim.2019.100546.
[35] A.M. Abdel-Ghany, I.M. Al-Helal, M.R. Shady, Human Thermal Comfort and Heat Stress in an Outdoor Urban Arid Environment: A Case Study, Advances in Meteorology 2013 (2) (2013), https://doi.org/10.1155/2013/693541.
[36] G.B. Anderson, M.L. Bell, Heat Waves in the United States: Mortality Risk during Heat Waves and Effect Modification by Heat Wave Characteristics in 43 U, S. Communities, Environmental Health Perspectves, 2011, pp. 210–218. 10.1289/ehp.1002313.
[37] C. Heaviside, S. Vardoulakis, X.M. Cai, Attribution of mortality to the urban heat island during heatwaves in the West Midlands, UK, Environ. Heal. A Glob. Access Sci. Source 15 (2016), https://doi.org/10.1186/s12940-016-0100-9.
[38] W.B. Goggins, E.Y. Chan, E. Ng, C. Ren, L. Chen, Effect Modification of the Association between Short- term Meteorological Factors and Mortality by Urban Heat Islands in Hong, Kong,PLoS One 7 (2012) 9–14. https://doi.org/10.1371/journal.pone.0038551.
[40] T. Asaeda, V.T. Ca, A. Wake, Heat storage of pavement and its effect on the lower atmosphere, Atmos. Environ. 30 (1996) 413–427, https://doi.org/10.1016/1352-2310(94)00140-5.
[41] J. He, A. Hoyano, Experimental study of cooling effects of a passive evaporative cooling wall constructed of porous ceramics with high water soaking-up ability, Build. Environ. 45 (2010) 461–472, https://doi.org/10.1016/j.buildenv.2009.07.002.

[42] E.L. Krüger, D. Pearlmutter, The effect of urban evaporation on building energy demand in an arid environment, Energy Build. 40 (2008) 2090–2098, https://doi.org/10.1016/j.enbuild.2008.06.002.
[43] T. Runsheng, Y. Etzion, E. Erell, Experimental studies on a novel roof pond configuration for the cooling of buildings, Renew. Energy 28 (2003) 1513–1522, https://doi.org/10.1016/S0960-1481(03)00002-8.
[44] E. Alexandri, P. Jones, Temperature decreases in an urban canyon due to green walls and green roofs in diverse climates, Build. Environ. 43 (2008) 480–493, https://doi.org/10.1016/j.buildenv.2006.10.055.
[45] H. Akbari, Shade trees reduce building energy use and CO_2 emissions from power plants, Environ. Pollut. 116 (2002) 119–126, https://doi.org/10.1016/S0269-7491(01)00264-0.
[46] S. Saneinejad, P. Moonen, J. Carmeliet, Comparative assessment of various heat island mitigation measures, Build. Environ. 73 (2014) 162–170, https://doi.org/10.1016/j.buildenv.2013.12.013.
[47] R. Levinson, H. Akbari, J.C. Reilly, Cooler tile-roofed buildings with near-infrared-reflective non-white coatings, Build. Environ. 42 (2007) 2591–2605, https://doi.org/10.1016/j.buildenv.2006.06.005.
[48] T. Karlessi, M. Santamouris, A. Synnefa, D. Assimakopoulos, P. Didaskalopoulos, K. Apostolakis, Development and testing of PCM doped cool colored coatings to mitigate urban heat island and cool buildings, Build. Environ. 46 (2011) 570–576, https://doi.org/10.1016/j.buildenv.2010.09.003.
[49] H. Takebayashi, M. Moriyama, Study on the urban heat island mitigation effect achieved by converting to grass-covered parking, Sol. Energy 83 (2009) 1211–1223, https://doi.org/10.1016/j.solener.2009.01.019.
[50] Ф.В. Тузиков, Ю.И. Рагино, Н.Л. Тузикова, М.В. Иванова, Р.В. ТалиМов, Ю.П. Никитин, Ф.В. Тузиков2, Ю.И. Рагино1, Нл. Тузикова2, М.В. Иванова1, Р.В. ТалиМов2, Ю.П. Никитин1, IEEE Int. Conf. Acoust. Speech, Signal Process. 2017. 41 (2017) 84–93.
[51] S. Menon, H. Akbari, S. Mahanama, I. Sednev, R. Levinson, Radiative forcing and temperature response to changes in urban albedos and associated CO_2 offsets, Environ. Res. Lett. 5 (2010), https://doi.org/10.1088/1748-9326/5/1/014005.
[52] T. Thongkanluang, N. Chirakanphaisarn, P. Limsuwan, Preparation of NIR reflective brown pigment, Procedia Eng. 32 (2012) 895–901, https://doi.org/10.1016/j.proeng.2012.02.029.
[53] S. Menon, H. Akbari, S. Mahanama, I. Sednev, R. Levinson, Radiative forcing and temperature response to changes in urban albedos and associated CO 2 offsets, Environmental Research, Letters 5 (2010), https://doi.org/10.1088/1748–9326/5/1/014005.
[54] N. Gaitani, G. Mihalakakou, M. Santamouris, On the use of bioclimatic architecture principles in order to improve thermal comfort conditions in outdoor spaces 42 (2007) 317–324, https://doi.org/10.1016/j.buildenv.2005.08.018.
[55] N. Anting, M.F.Md Din, K. Iwao, M. Ponraj, K. Jungan, L.Y. Yong, A.J.L.M. Siang, Experimental evaluation of thermal performance of cool pavement material using waste tiles in tropical climate, Energy Build. 142 (2017) 211–219, https://doi.org/10.1016/j.enbuild.2017.03.016.
[56] H. Li, J. Harvey, A. Kendall, Field measurement of albedo for different land cover materials and effects on thermal performance 59 (2013) 536–546, https://doi.org/10.1016/j.buildenv.2012.10.014.
[57] A. Synnefa, T. Karlessi, N. Gaitani, M. Santamouris, D.N. Assimakopoulos, C. Papakatsikas, Experimental testing of cool colored thin layer asphalt and estimation of its potential to improve the urban microclimate, Build. Environ. 46 (2011) 38–44, https://doi.org/10.1016/j.buildenv.2010.06.014.
[58] T. Karlessi, M. Santamouris, K. Apostolakis, A. Synnefa, I. Livada, Development and testing of thermochromic coatings for buildings and urban structures, Sol. Energy 83 (2009) 538–551, https://doi.org/10.1016/j.solener.2008.10.005.
[59] E. Mushtaha, S. Shareef, I. Alsyouf, T. Mori, A. Kayed, M. Abdelrahim, S. Albannay, A study of the impact of major urban heat island factors in a hot climate courtyard: The case of the University of Sharjah, UAE, Sustain. Cities Soc. 69 (2021), 102844, https://doi.org/10.1016/j.scs.2021.102844.
[60] A. Forouzandeh, Prediction of surface temperature of building surrounding envelopes using holistic microclimate ENVI-met model, Sustain. Cities Soc. 70 (2021), 102878, https://doi.org/10.1016/j.scs.2021.102878.
[61] M. Unal Cilek, A. Cilek, Analyses of land surface temperature (LST) variability among local climate zones (LCZs) comparing Landsat-8 and ENVI-met model data, Sustain. Cities Soc. 69 (2021), 102877, https://doi.org/10.1016/j.scs.2021.102877.
[62] B. Paas, C. Schneider, A comparison of model performance between ENVI-met and Austal2000 for particulate matter, Atmos. Environ. 145 (2016) 392–404, https://doi.org/10.1016/j.atmosenv.2016.09.031.
[63] E. Najaf, H. Abbasi,Using Recycled Concrete Powder, Waste Glass Powder, and Plastic Powder to Improve the Mechanical Properties of Compacted Concrete: Cement Elimination Approach, Advances in Civil Engineering, 1 (2022), doi:DOI: 10.1155/2022/9481466.
[64] M. Orouji, S.M. Zahrai, E. Najaf, Effect of glass powder & polypropylene fibers on compressive and flexural strengths, toughness and ductility of concrete: an environmental approach, Structures 33 (2021) 4616–4628, https://doi.org/10.1016/j.istruc.2021.07.048.
[65] E. Najaf, H. Abbasi, S.M. Zahrai, Effect of waste glass powder, microsilica and polypropylene fibers on ductility, flexural and impact strengths of lightweight concrete, Int. J. Struct. Integr. 13 (2022) 511–533, https://doi.org/10.1108/IJSI-03-2022-0039.
[66] R. Levinson, H. Akbari, Effects of composition and exposure on the solar reflectance of portland cement concrete, Cem. Concr. Res. (2002), https://doi.org/10.1016/S0008-8846(02)00835-9.
[67] A. Baral, S. Sen, J.R. Roesler, Use phase assessment of photocatalytic cool pavements, J. Clean. Prod. 190 (2018) 722–728, https://doi.org/10.1016/j.jclepro.2018.04.155.
[68] H. Li, J.T. Harvey, T.J. Holland, M. Kayhanian, Erratum: The use of reflective and permeable pavements as a potential practice for heat island mitigation and stormwater management (Environ. Res. Lett. (2013) 8 (015023)), Environ. Res. Lett. 8 (2013), https://doi.org/10.1088/1748-9326/8/4/049501.
[69] V. Di Maria, M. Rahman, P. Collins, G. Dondi, C. Sangiorgi, Urban heat Island effect: thermal response from different types of exposed paved surfaces, Int. J. Pavement Res. Technol. 6 (2013) 414–422, https://doi.org/10.6135/ijprt.org.tw/2013.6(4).414.
[70] G. Torgal, P.F.; Labrincha, J.A.; Cabeza, L.F.; Granqvist, Eco-Efficient Materials for Mitigating Building Cooling Needs, 2016. https://doi.org/10.1016/c2014–0-02697–4.
[71] F. Salata, I. Golasi, A.D.L. Vollaro, R.D.L. Vollaro, How high albedo and traditional buildings' materials and vegetation affect the quality of urban microclimate. A case study, Energy Build. 99 (2015) 32–49, https://doi.org/10.1016/j.enbuild.2015.04.010.
[72] F. Salata, I. Golasi, R. de Lieto Vollaro, A. de Lieto Vollaro, Urban microclimate and outdoor thermal comfort. A proper procedure to fit ENVI-met simulation outputs to experimental data, Sustain. Cities Soc. 26 (2016) 318–343, https://doi.org/10.1016/j.scs.2016.07.005.
[73] N.L. Alchapar, E.N. Correa, The use of reflective materials as a strategy for urban cooling in an arid "OASIS" city, Sustain. Cities Soc. 27 (2016) 1–14, https://doi.org/10.1016/j.scs.2016.08.015.
[74] D.D. Kolokotsa, G. Giannariakis, K. Gobakis, G. Giannarakis, A. Synnefa, M. Santamouris, Cool roofs and cool pavements application in Acharnes, Greece, Sustain. Cities Soc. 37 (2018) 466–474, https://doi.org/10.1016/j.scs.2017.11.035.
[75] G.E. Kyriakodis, M. Santamouris, Using reflective pavements to mitigate urban heat island in warm climates - results from a large scale urban mitigation project, Urban Clim. 24 (2018) 326–339, https://doi.org/10.1016/j.uclim.2017.02.002.
[76] S.G. Williams, Construction of roller-compacted concrete pavement in the Fayetteville Shale Play Area, Arkansas, Transp. Res. Rec. J. Transp. Res. Board (2014), https://doi.org/10.3141/2408-06.
[77] D. Jones, J. Harvey, I.L. Al-Qadi, A. MAteos, Advances in Pavement Design through Full-scale Accelerated Pavement Testing. https://doi.org/10.1201/b13000.
[78] Department of The Army U.S. Army Corps of Engineers, Engineering and Design ROLLER-COMPACTED CONCRETE, 2006.
[79] S. Alper, B.A. Tayeh, M. Uzun, The evaluation of calcium carbonate added and basalt fiber reinforced roller compacted high performance concrete for pavement case studies in construction materials, Case Stud. Constr. Mater. 17 (2022), e01293, https://doi.org/10.1016/j.cscm.2022.e01293.
[80] V. Hospodarova, J. Junak, N. Stevulova, Color pigments in concrete and their properties, Pollack Period 10 (2015) 143–151, https://doi.org/10.1556/606.2015.10.3.15.
[81] A. López, J.M. Tobes, G. Giaccio, R. Zerbino, Advantages of mortar-based design for coloured self-compacting concrete, Cem. Concr. Compos. 31 (2009) 754–761, https://doi.org/10.1016/j.cemconcomp.2009.07.005.

[82] M. Uysal, The use of waste maroon marble powder and iron oxide pigment in the production of coloured self-compacting concrete, Adv. Civ. Eng. (2018) (2018), https://doi.org/10.1155/2018/8093576.
[83] M.Z. Heerah, I. Galobardes, G. Dawson, Characterisation and control of cementitious mixes with colour pigment admixtures, Case Stud. Constr. Mater. 15 (2021), e00571, https://doi.org/10.1016/j.cscm.2021.e00571.
[84] K. Inoue, K. Hara, K. Urahama, Spectral reflectance estimation and color reproduction based on sparse Neugebauer model, Adv. Sci. Technol. Eng. Syst. 2 (2017) 958–966, https://doi.org/10.25046/aj0203121.
[85] ASTM C1170/C1170M - 14, ASTM C1170, Standard Test Method for Determining Consistency and Density of Roller-Compacted Concrete Using a Vibrating Table 1, ASTM Int. 91 (2014).
[86] C.C. Test, T. Drilled, C.C. Test, B. Statements, ASTM C 39/C 39M – 01. Standard Test Method for Compressive Strength of Cylindrical Concrete Specimens, (2014) 3–9. https://doi.org/10.1520/C0039.
[87] ASTM C496/C496M – 17, Standard Test Method for Splitting Tensile Strength of Cylindrical Concrete Specimens ASTM C-496, ASTM Int. (2011) 1–5. ftp://ftp.astmtmc.cmu.edu/docs/diesel/cummins/procedure_and_ils/ism/Archive/ISM Procedure (Draft 10).doc.
[88] ACPA (American Concrete Pavement Association), Roller-Compacted Concrete Guide Specificaiton, (2014) 1–29.
[89] M. Chi, R. Huang, Effect of circulating fluidized bed combustion ash on the properties of roller compacted concrete, Cem. Concr. Compos. 45 (2014) 148–156, https://doi.org/10.1016/j.cemconcomp.2013.10.001.
[90] M.N.T. Lam, D.H. Le, S. Jaritngam, Compressive strength and durability properties of roller-compacted concrete pavement containing electric arc furnace slag aggregate and fly ash, Constr. Build. Mater. 191 (2018) 912–922, https://doi.org/10.1016/j.conbuildmat.2018.10.080.
[91] J. LaHucik, S. Dahal, J. Roesler, A.N. Amirkhanian, Mechanical properties of roller-compacted concrete with macro-fibers, Constr. Build. Mater. 135 (2017) 440–446, https://doi.org/10.1016/j.conbuildmat.2016.12.212.
[92] F. Vahedifard, M. Nili, C.L. Meehan, Assessing the effects of supplementary cementitious materials on the performance of low-cement roller compacted concrete pavement, Constr. Build. Mater. 24 (2010) 2528–2535, https://doi.org/10.1016/j.conbuildmat.2010.06.003.
[93] E. Rahmani, M.K. Sharbatdar, M. H.A.Beygi, A comprehensive investigation into the effect of water to cement ratios and cement contents on the physical and mechanical properties of Roller Compacted Concrete Pavement (RCCP, Constr. Build. Mater. 253 (2020), 119177, https://doi.org/10.1016/j.conbuildmat.2020.119177.
[94] C. Cao, W. Sun, H. Qin, Analysis on strength and fly ash effect of roller-compacted concrete with high volume fly ash, Cem. Concr. Res. 30 (2000) 71–75, https://doi.org/10.1016/S0008-8846(99)00203-3.
[95] S. Saluja, S. Goyal, B. Bhattacharjee, Strength properties of roller compacted concrete containing GGBS as partial replacement of cement, J. Eng. Res. 7 (2019) 1–17.
[96] Y. Abut, S. Taner Yildirim, Structural design and economic evaluation of roller compacted concrete pavement with recycled aggregates, IOP Conf. Ser. Mater. Sci. Eng. 245 (2017), https://doi.org/10.1088/1757-899X/245/2/022064.
[97] H.E. Fardin, A.G. dos Santos, Roller compacted concrete with recycled concrete aggregate for paving bases, Sustainability 12 (2020), https://doi.org/10.3390/SU12083154.
[98] C. Chhorn, S.J. Hong, S.W. Lee, ScienceDirect Relationship between compressive and tensile strengths of roller-compacted concrete, in: J. Traffic Transp. Eng., 5, 2017, pp. 215–223, https://doi.org/10.1016/j.jtte.2017.09.002.
[99] O. Çalışkan, B. Sakar, Design for mitigating urban heat island: proposal of a parametric model, Iconarp Int. J. Archit. Plan 7 (2019) 158–181, https://doi.org/10.15320/iconarp.2019.84.
[100] F. CANAN, Kent Geometrisine Bağlı Olarak Kentsel Isı Adası Etkisinin Belirlenmesi: Konya Örneği, Çukurova Üniversitesi Mühendislik-Mimar. Fakültesi Derg. (2017) 69–80, https://doi.org/10.21605/cukurovaummfd.357202.
[101] E. Kocak, Kentsel Yayılmanın, Yerel İklim Değişikliği Üzerine Etkilerinin Sıcaklık Ve Yağış Parametreleri Üzerinden Değerlendirilmesi: Konya İli Örneği, MAS Journal of Applied Sciences 7 (2) (2022) 452–473, https://doi.org/10.52520/masjaps.v7i2id197.
[102] D.J. Sailor, S.M.A. Suite, Evaluating the ENVI-met microscale model for suitability in analysis of targeted urban heat mitigation strategies, Urban Clim. 26 (2018) 188–197.
[103] M. Sule Zango, L. Yaik Wah, D. Hooi Chyee, A. Dalandi, Validation of envi-met software using measured and predicted air temperatures in the courtyard of Chinese Shophouse Malacca, J. Appl. Sci. Environ. Sustain. 4 (2018) 28–36.
[104] D. Ambrosini, G. Galli, B. Mancini, I. Nardi, S. Sfarra, Evaluating mitigation effects of urban heat islands in a historical small center with the ENVI-Met® climate model, Sustainability 6 (2014) 7013–7029, https://doi.org/10.3390/su6107013.
[105] M. Performance, N.I. Spectrophotom-, A. Mass, Z. Solar, I. Tables, S. Materials, U. Sunlight, Standard Test Method for Solar Absorptance, Reflectance, and Transmittance of Materials Using Integrating Spheres 1, 03 (1996) 1–9.
[106] P. Conry, A. Sharma, M.J. Potosnak, L.S. Leo, E. Bensman, J.J. Hellmann, H.J.S. Fernando, Chicago's heat island and climate change: Bridging the scales via dynamical downscaling, Journal of Applied Meteorology and Climatology 54 (2015) 1430–1448, https://doi.org/10.1175/JAMC-D-14-0241.1.
[107] M. Shams. Western Urban Heat Mitigation for Current and Future Conditions: A case study for downtown London ON,, The University of Westedn Ontario, 2021.
[108] T. Sharmin, K. Steemers, A. Matzarakis, Microclimatic modelling in assessing the impact of urban geometry on urban thermal environment, Sustain. Cities Soc. 34 (2017) 293–308, https://doi.org/10.1016/j.scs.2017.07.006.
[109] M. Taleghani, U. Berardi, The effect of pavement characteristics on pedestrians' thermal comfort in Toronto, Urban Clim. 24 (2018) 449–459, https://doi.org/10.1016/j.uclim.2017.05.007.
[110] L. Battistella, M. Noro, Urban heat island in Padua, Italy: simulation analysis and mitigation strategies, Build. Simul. Appl. (2015) 99–107.
[111] C. Huynh, R. Eckert, Reducing heat and improving thermal comfort through urban design – a case study in Ho Chi Minh City, Int. J. Environ. Sci. Dev. 3 (2012) 480–485, https://doi.org/10.7763/ijesd.2012.v3.271.
[112] F. Salata, I. Golasi, A.D.L. Vollaro, R.D.L. Vollaro, How high albedo and traditional buildings' materials and vegetation affect the quality of urban microclimate. A case study, Energy Build. 99 (2015) 32–49, https://doi.org/10.1016/j.enbuild.2015.04.010.
[113] J. Li, B. Zheng, N.H. Wong, X. Ouyang, Does shrub benefit the thermal comfort at pedestrian height in Singapore ? Sustain. Cities Soc. (2021), 103333 https://doi.org/10.1016/j.scs.2021.103333.
[114] M. Hendel, P. Gutierrez, M. Colombert, Y. Diab, L. Royon, Measuring the effects of urban heat island mitigation techniques in the field: Application to the case of pavement-watering in Paris, Urban Clim. 16 (2016) 43–58, https://doi.org/10.1016/j.uclim.2016.02.003.
[115] C. Rosenzweig, W. Solecki, L. Parshall, S. Gaffin, B. Lynn, R. Goldberg, J. Cox, S. Hodges, Mitigating New York City's heat island with urban forestry, living roofs, and light surfaces, In: Proceedings of the 86th AMS Annual Meeting. 2006.
[116] U. Berardi, Z. Jandaghian, J. Graham, Effects of greenery enhancements for the resilience to heat waves: A comparison of analysis performed through mesoscale (WRF) and microscale (Envi-met) modeling, Sci. Total Environ. 747 (2020), 141300, https://doi.org/10.1016/j.scitotenv.2020.141300.
[117] V. Lontorfos, C. Efthymiou, M. Santamouris, On the time varying mitigation performance of reflective geoengineering technologies in cities, Renew. Energy 115 (2018) 926–930, https://doi.org/10.1016/j.renene.2017.09.033.
[118] J. Yang, Z.H. Wang, K.E. Kaloush, Environmental impacts of reflective materials: Is high albedo a "silver bullet" for mitigating urban heat island? Renew. Sustain. Energy Rev. 47 (2015) 830–843, https://doi.org/10.1016/j.rser.2015.03.092.